*2nd URSI AT-RASC, Gran Canaria, 28 May – 1 June 2018*

# A Comparative Analysis of Strong Scintillation I: Configuration-Space Simulations

Charles L. Rino*(1),Charles S. Carrano(1), Nicolay N. Zernov(2), and Vadim E. Germ(2)
(1) Institute for Scientific Research, Boston College, USA
(2) University of St. Petersburg, St. Petersburg, Russia

## Abstract

The parabolic wave equation (PWE) characterizes the interaction of propagating electromagnetic waves with the ionosphere. Equatorial plasma bubble (EPB) environments are particularly challenging because they present an extended highly inhomogeneous, anisotropic, structure. It is generally assumed that developed intermediate-scale structure can be characterized by a spectral density function (SDF). However, structured regions that are sufficient homogeneous to support an SDF characterization are embedded in larger background structures that define EPBs

Numerical simulations of the propagation of an electromagnetic wave in an EPB environment generate realizations that potentially accommodate both background and stochastic components of the environment. However, this presupposes that one has a good representation of the environment. Furthermore, the objective is to obtain tractable characterizations of observables that can be used for remote ionospheric sensing and evaluating or predicting the effects of propagation disturbances on satellite communication and navigation systems. Recent studies by Zernov and Gherm [1 - 3] have addressed these issues within the framework of hybrid analytical solutions to the problem.

An alternative approach to the problem by Carrano and Rino [4] uses an equivalent phase screen, effectively to absorb the complexity of the EPB environment. Further simplification is achieved by constraining the propagation effects to a two-dimensional plane defined by the propagation vector and the scan direction defined by the translation of the propagation vector through the medium. The results are supported by an exact solution of the PWE for two-dimensional propagation of the field created by a two-component inverse-power-law phase SDF. The equivalent-phase-screen theory provides complete characterization of any intensity scintillation record in terms of 5 parameters. The best-fit parameters can be determined by the irregularity parameter estimation (IPE) procedure described in Carrano and Rino [4].

This paper and a companion paper by Gherm, Zernov and Rino present a comparative analysis of the two approaches. Common configuration-space structure realizations with specified two-component inverse-power-law SDFs are used for the comparisons. The parameters selected for comparison were derived from analysis of high-resolution EPB simulation by Yokoyama [5].

## 1 Configuration-Space Models

Configuration-space models use scale-dependent field-aligned structure elements referred to as striations. The structure can be an ionization enhancement or a void in a background structure. Let $\zeta_s - \zeta_s^k$ represent distance along the $k^{\text{th}}$ field line. The initiation point is placed in a cross-field. Vector components parallel and normal to the field line in the plane of curvature, namely $\zeta_\parallel^k$, and $\zeta_\perp^k$, can be constructed at any point along a field line. Striations shapes are defined by monotonically decreasing functions of either distance along the field line, $p_s(\zeta)$, or radial distance, $p_\perp(|\zeta|)$. The defining equation for a striation includes a fractional strength parameter, $F_k$:

$$\begin{aligned}\Delta N_k(\zeta_s,\zeta_\tau)/N_0 &= F_k p_s(\left|\zeta_s-\zeta_s^k\right|/\sigma_s)\\ &\times\ p_\perp(\left|\zeta_\tau-\zeta_\tau^k\right|/\sigma_k).\end{aligned}\qquad(1)$$

The parameter $\sigma_k$ determines the cross-field dimension or scale of the striation. A complete structure realization is generated by summing the contributions striations with specified fractional strengths, $F_k$, sizes, $\sigma_k$ and reference locations $\zeta_s^k$ and $\zeta_\tau^k$:

$$\begin{aligned}\Delta N(\zeta_s,\zeta_\tau)/N_0 &= \frac{1}{N_s}\sum_k F_k p_s(\left|\zeta_s-\zeta_s^k\right|/\sigma_s)\\ &\times\ p_\perp(\left|\zeta_\tau-\zeta_\tau^k\right|/\sigma_k),\end{aligned}\qquad(2)$$

where $N_s$ is the total number of striations.

Successive bifurcation is often invoked to describe the EPB structuring. Steep gradients are broken up by generating depletions flanked by higher density regions. Each new structure component bifurcates similarly, forming a structure cascade. Successive bifurcation is captured by the following scaling relation for $\sigma_j$ and the number of striations at each scale:

$$\begin{aligned}\sigma_j &= \sigma_{\max}2^{-(J_{\max}-j)}\\ N_j &= 2^{d-j}\end{aligned}\quad \text{for } j=1,2,\cdots,J_{\max}.\qquad(3)$$

The parameter $d$ defines the number of striations at the largest scale. The total number of striations is $N_s = \sum_j N_j$. To complete the configuration-space definition we let

$$F_k = C_s \sigma_k^{\gamma}. \tag{4}$$

The spectral density function of the realization is given as

$$\left\langle |\Delta N(\kappa_s)|^2 \right\rangle / N_0^2 = \frac{C_s}{NF \cdot N_s} \left[ \sum_{j=J_{\min}}^{J_{\max}} N_j \sigma_j^{2\gamma_1+1} \left| \widehat{p}_{\perp}^{(1)}(\kappa_s \sigma_j) \right|^2 + CF \sum_{j=J_{\min}}^{J_{\max}} N_j \sigma_j^{2\gamma_2+1} \left| \widehat{p}_{\perp}^{(1)}(\kappa_s \sigma_j) \right|^2 \right] \tag{5}$$

The parameter $CF$ is chosen to maintain continuity at the break scale.

## 2 Configuration-Space Realizations

It is generally accepted that observable one-dimensional electron density SDFs with sufficient homogeneity can be characterized by the two-component inverser-power-law form

$$\Phi_{N_e}(q_y) = C_s \begin{cases} q^{-\eta_1} & \text{for } q \le q_0 \\ q_0^{\eta_2-\eta_1} q^{-\eta_2} & \text{for } q > q_0 \end{cases} \tag{6}$$

The spatial wavenumber range is dictated by the duration of the data segment, $L$ and the sampling interval $\Delta y$:

$$2\pi/L \le q \le 2\pi/\Delta y. \tag{7}$$

Figure 1 shows the predicted one-dimensional SDF from (2). A realization of the structure generated by (1) is shows in Figure 2.

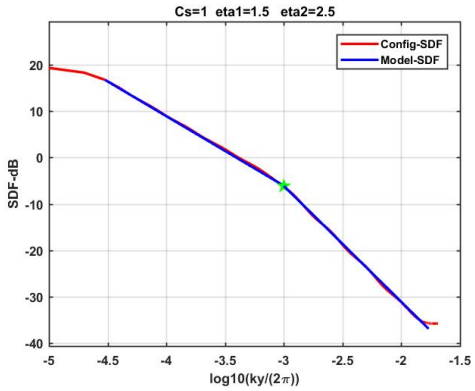


**Figure 1.** Example of two-component SDF predicted by 4

.

While there is considerable evidence that supports the model as representative of measured in-situ structure or structure derived from the analysis of scintillation data, the uniform environment shown in Figure 2 is highly idealized. For example, Figure 3 is a cross-field structure realization derived from new high resolution simulations by Yokoyama [5]. More than just a simple overall weighting with background density, the the spectral characteristics vary. Because the configuration space model is generated in configuration space, it is straightforward to impose

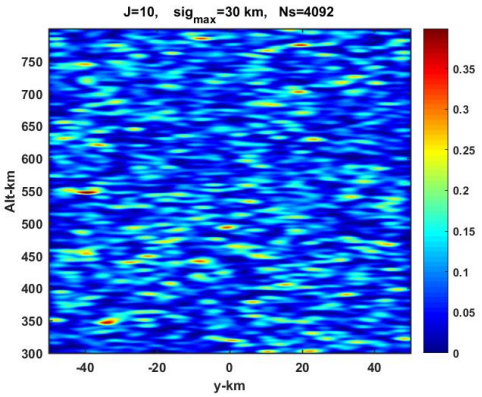


**Figure 2.** Two-dimensional cross-field structure realization

.

height-dependent structure variations. Figure 4, for example shows a cross-field realization with structure scaled to the average background electron density show in the right frame of Figure 2.

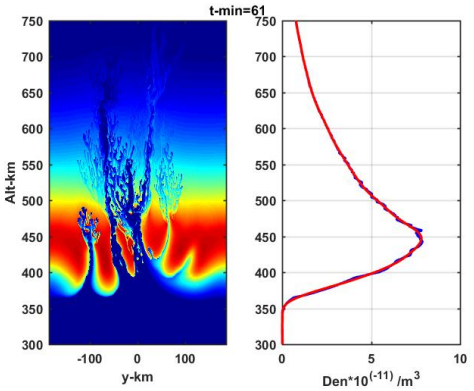


**Figure 3.** Physics based EPB realization

.

## 3 Discussion

A comparison of Figures 4 and Figures 2 emphasize a characteristic of stochastic models, namely that the zonal structure variation is lost, while preserving the average scale distribution. Indeed, one-dimensional SDF measurements are statistically similar. It should also be noted that the stochastic variation is determined by the random distribution of the striation locations. Oblique slice planes will reflet the projection for the elongated striations until field-aligned measurements will be dominated, at least in terms of diffraction effects, by the shape of the striations. Current models assume uniformity and ignore field-line curvature.

The ramifications for propagation present considerable challenges. The configuration-space model offers a consistent definition of structure derived from a two-dimensional stochastic model an isotropic inverse-power-law configuration. These are all details that can be varied and compared to measurement. The model is particularly relevant to the

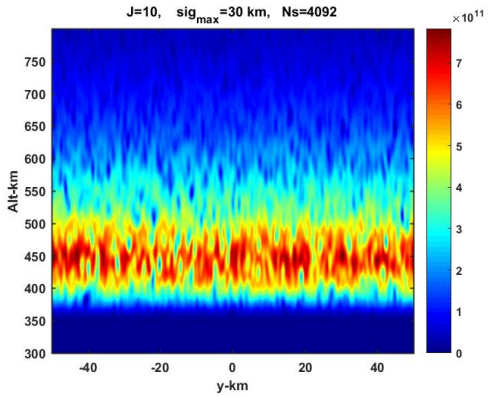


**Figure 4.** Configuration space cross-field realization with imposed height variation.

.

interpretation of GPS low-earth-orbiting satellite occultation measurements Tsai [6].

## References


[1] N. N. Zernov, V. E. Gherm, and H. J. Strangeways, "On the effects of scintillation of low-latitude bubbles on transionospheric paths of propagation," *Radio Science*, **44**,1, 2009, doi:10.1029/2008RS004074.

[2] N. N. Zernov, V. E. Gherm, and H. J. Strangeways, "Further determinations of strong scintillation effects on GNSS signals using the Hybrid Scintillation Propagation Model," Radio Science, **47**,4, 2012, pp. 2–7, doi:10.1029/2011RS004935.

[3] N. N. Zernov, V. E. Gherm, and H. J. Strangeways, "Extension of Hybrid Scintillation Propagation Model to the case of field propagation in the ionosphere with highly anisotropic irregularities," *Radio Science*, **52**,7, 2012, pp. 874-883, 2017, doi: 10.1002/2017RS006264.

[4] C.S. Carrano and C.L. Rino, "A theory of scintillation for two-component power law irregularity spectra: Overview and numerical results," *Radio Science*, **52**, 51, 6, 2016, pp. 789-813, doi:10.1002/2015RS005841.

[5] T. Yokoyama, "A review on the numerical simulation of equatorial plasma bubbles toward scintillation evaluation and forecasting," *Progress in Earth and Planetary Science*, **4**,1, 2017, doi:10.1186/s40645-017-0153-6.

[6] L. C. Tsai, , , K. C. Cheng, C. H. Liu, "GPS radio occultation measurements on ionospheric electron density from low earth orbit," *Journal of Geodesy*, **85**,1, 2011, pp. 7421–7428.